HHS Public Access

Author manuscript

Immunity. Author manuscript; available in PMC 2017 August 16.

Published in final edited form as:

Immunity. 2016 August 16; 45(2): 389–401. doi:10.1016/j.immuni.2016.07.011.

Tumor-Specific T Cell Dysfunction Is a Dynamic Antigen-Driven Differentiation Program Initiated Early during Tumorigenesis

Andrea Schietinger[1,2,3,11,*], **Mary Philip**[1,4,11], **Varintra E. Krisnawan**[1,2], **Edison Y. Chiu**[2], **Jeffrey J. Delrow**[5], **Ryan S. Basom**[5], **Peter Lauer**[6], **Dirk G. Brockstedt**[6], **Sue E. Knoblaugh**[7,12], **Günter J. Hämmerling**[8], **Todd D. Schell**[9], **Natalio Garbi**[8,10], and **Philip D. Greenberg**[2,3,*]

[1]Immunology Program, Memorial Sloan Kettering Cancer Center, New York, NY 10065, USA

[2]Department of Immunology, University of Washington, Seattle, WA 98109, USA

[3]Program of Immunology, Fred Hutchinson Cancer Research Center, Seattle, WA 98109, USA

[4]Division of Hematology, University of Washington, Seattle, WA 98195, USA

[5]Genomics and Bioinformatics Shared Resources, Fred Hutchinson Cancer Research Center, Seattle, WA 98109, USA

[6]Aduro BioTech, Inc., Berkeley, CA 94710, USA

[7]Comparative Medicine Shared Resource, Fred Hutchinson Cancer Research Center, Seattle, WA 98109, USA

[8]Divisions of Cellular and Molecular Immunology, DKFZ, 69120 Heidelberg, Germany

[9]Department of Microbiology & Immunology, Penn State Hershey College of Medicine, Hershey, PA 17033, USA

[10]Institutes of Molecular Medicine and Experimental Immunology, University of Bonn, 53127 Bonn, Germany

SUMMARY

CD8$^+$ T cells recognizing tumor-specific antigens are detected in cancer patients but are dysfunctional. Here we developed a tamoxifen-inducible liver cancer mouse model with a defined

[*]Correspondence: schietia@mskcc.org (A.S.), pgreen@uw.edu (P.D.G.).

[11]Present address: Memorial Sloan Kettering Cancer Center, Immunology Program, 1275 York Avenue, Box 512, New York, NY 10065, USA

[12]Present address: Department of Veterinary Biosciences, The Ohio State University, Columbus, OH 43210, USA

AUTHOR CONTRIBUTIONS

A.S. conceived and designed the study, carried out experiments, interpreted data, and wrote the manuscript. M.P. performed experiments, generated and analyzed data, and contributed to manuscript writing. V.E.K. and E.Y.C. performed experiments. J.J.D. and R.S.B. carried out microarray data analysis. D.G.B. and P.L. generated *Listeria* strains. T.D.S. provided advice. S.E.K. reviewed histology of liver sections. G.J.H., N.G., and T.D.S. provided mice. P.D.G. conceived the study and wrote the manuscript.

ACCESSION NUMBERS

The microarray data have been deposited in the Gene Expression Omnibus under accession number GEO: GSE60501.

SUPPLEMENTAL INFORMATION

Supplemental Information includes seven figures, four tables, and Supplemental Experimental Procedures and can be found with this article online at http://dx.doi.org/10.1016/j.immuni.2016.07.011.

oncogenic driver antigen (SV40 large T-antigen) to follow the activation and differentiation of naive tumor-specific CD8$^+$ T (TST) cells after tumor initiation. Early during the pre-malignant phase of tumorigenesis, TST cells became dysfunctional, exhibiting phenotypic, functional, and transcriptional features similar to dysfunctional T cells isolated from late-stage human tumors. Thus, T cell dysfunction seen in advanced human cancers may already be established early during tumorigenesis. Although the TST cell dysfunctional state was initially therapeutically reversible, it ultimately evolved into a fixed state. Persistent antigen exposure rather than factors associated with the tumor microenvironment drove dysfunction. Moreover, the TST cell differentiation and dysfunction program exhibited features distinct from T cell exhaustion in chronic infections. Strategies to overcome this antigen-driven, cell-intrinsic dysfunction may be required to improve cancer immunotherapy.

In Brief

Tumor-specific CD8$^+$ T cells found in human solid tumors are often dysfunctional, but when and how during tumorigenesis this T cell dysfunction arises was not known. Schietinger and colleagues show that CD8$^+$ T cells become dysfunctional early during tumorigenesis at the pre-malignant stage through an antigen-driven dynamic differentiation program.

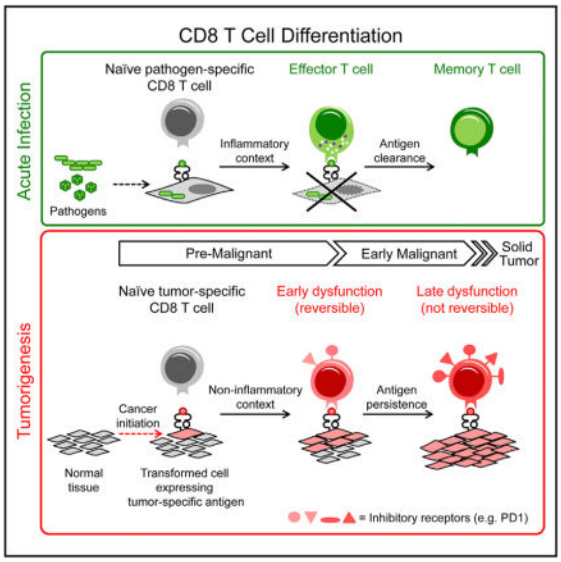

INTRODUCTION

T cell responses to cancers differ depending on the target antigen (Schietinger et al., 2008). Tumor antigens that are self-proteins are often weakly immunogenic due to pre-existing tolerance. Tolerance to self results from both central and peripheral immune tolerance mechanisms and is required to prevent autoimmunity (Schietinger and Greenberg, 2014). However, many cancer antigens are self-antigens, and tolerance to these proteins can impede anti-tumor T cell responses. In contrast, tumor antigens that are truly tumor specific (viral and mutated proteins) are potentially highly immunogenic because the immune system has not been previously exposed to these antigens, and T cells should be able to recognize these

neoantigens as “foreign” and eliminate cancer cells expressing them (Schietinger et al., 2008). Mutant antigens are commonly expressed in human solid tumors (Alexandrov et al., 2013), and T cells specific for such antigens are detected in cancer patients (Kubuschok et al., 2006; Lennerz et al., 2005; Linnemann et al., 2015; Robbins et al., 1996; Wölfel et al., 1995). However, the co-existence of progressively growing tumors and tumor-specific T cells, first defined as the “Hellstrom paradox,” suggests that tumor-specific T cells are rendered unresponsive to the cancer (Hellström et al., 1968). Tumor-infiltrating lymphocytes (TILs) within progressing, solid tumors and metastatic lesions commonly express high amounts of inhibitory receptors (e.g., PD1, LAG3, 2B4, TIM3, CTLA4), are impaired in the ability to produce effector cytokines (TNF-α, IFN-γ, and IL-2), and/or have lost the capacity to proliferate (Baitsch et al., 2011; Gros et al., 2014; Gubin et al., 2014). These hallmarks of dysfunction have been attributed to factors within established tumors, including the immunosuppressive microenvironment (e.g., myeloid-derived suppressor cells [Gabrilovich et al., 2012], tumor-associated macrophages [Noy and Pollard, 2014], $FOXP3^+$ regulatory $CD4^+$ T cells [Savage et al., 2013], IL-10, TGF-β, indoleamine-2,3 dioxygenase [IDO]), inhibitory checkpoint signaling pathways (e.g., PD1 and PD-L1) (Ostrand-Rosenberg et al., 2014), and physiological changes (e.g., hypoxia and low nutrient levels).

Tumor development occurs in three phases: initiation, promotion, and progression. During initiation, normal cells acquire somatic (driver) mutations that induce neoplastic transformation. After the initiating oncogenic hit, there is a pre-malignant phase during which tumor-specific neoantigens, including mutant oncogenic driver antigens, may be expressed and presented to the immune system in a non-inflammatory context (Willimsky and Blankenstein, 2005). It is currently not known when and how tumor-specific $CD8^+$ T cells differentiate to an unresponsive state. Defining the underlying mechanisms and kinetics of differentiation to the dysfunctional state requires following naive tumor-specific T cells from the earliest time after tumor initiation through the course of tumor development; this is impossible to study in human patients or in transplantable tumor models. Thus, we set out to develop an inducible, autochthonous cancer mouse model with a defined tumor-specific oncogenic driver that represents a tumor-specific $CD8^+$ T cell target (neoantigen), and we followed the activation and differentiation of tumor-specific T cells after tumor initiation. Our study reveals that the phenotypic, functional, and molecular hallmarks of unresponsive tumor-specific $CD8^+$ T cells found in late-stage tumors are already “imprinted” through a dynamic differentiation program at the pre- and early malignant phase of tumor development, prior to the development of an established tumor and/or immunosuppressive microenvironment. Moreover, fate commitment to the dysfunctional state absolutely required continuous antigen encounter and TCR stimulation.

RESULTS

A Tumor-Specific Neoantigen Expressed Early during Tumorigenesis Rapidly Induces Unresponsiveness in Antigen-Specific $CD8^+$ T Cells

To follow the fate of naive tumor-specific $CD8^+$ T cells during the subclinical, pre-malignant phase of tumor development, we developed a tamoxifen-inducible, autochthonous liver cancer model (ASTxCre-ER^{T2}; AST = Albumin-floxStop-SV40 large T antigen [Stahl et al.,

2009]; Cre-ER^{T2} = tamoxifen-dependent Cre-recombinase) with the induced expression of SV40 large T antigen (Tag) serving as both oncogenic driver and tumor-specific antigen (Figure 1A). Tag mediates its transforming activity through the binding and functional inactivation of two central tumor suppressor proteins, retinoblastoma protein and the p53 transcription factor, similar to oncogenes in human cancers. Tamoxifen (Tam)-treated ASTxCre-ER^{T2} mice show morphologic alterations in the liver by days 8–10; these lesions, defined pathologically as pre- and early malignant through ~day 30 (Cullen et al., 1993; Thomas et al., 2005), eventually progress into frank hepatocellular carcinoma (HCC) by 3–4 months after Tam (Figures 1B and S1A), with all mice succumbing to HCC by 4–5 months (Figure S1B). TCR$_{SV40\text{-}I}$ transgenic mice, which have monoclonal CD8$^+$ T cells expressing a D^b-restricted TCR specific for Tag epitope I (Tag-I; SAINNYAQKL), were used as the source of naive tumor-specific CD8$^+$ T cells (Figure 1C; Staveley-O'Carroll et al., 2003). CD8$^+$ T cells isolated from spleens of TCR$_{SV40\text{-}I}$ mice were phenotypically and functionally naive and after transfer into B6 mice proliferated and differentiated into functional effector and memory T cells in response to an acute infection, e.g., immunization with a recombinant *Listeria monocytogenes* strain expressing the Tag epitope I (LM-Tag-I) in which the pathogen and antigen are rapidly and effectively cleared (Figure 1D; Brockstedt et al., 2004; Cui and Kaech, 2010).

To understand how naive tumor-specific CD8$^+$ T cells differentiate and respond to first encountering a tumor-specific antigen early during tumor development, we transferred naive TCR$_{SV40\text{-}I}$ CD8$^+$ T cells into congenic ASTxCre-ER^{T2} mice 1–2 days prior to Tam treatment (Figure 1E) and assessed phenotype and function at different time points after Tam. By 3–4 days after Tam, TCR$_{SV40\text{-}I}$ infiltrated the liver, proliferated, and became antigen experienced as evidenced by proliferation-induced dilution of carboxy-fluorescein-succinimidyl ester (CFSE) and acquisition of a CD44^{hi} phenotype (Figure 1F). By days 8–10, TCR$_{SV40\text{-}I}$ CD8$^+$ T cells (D8 TCR$_{SV40\text{-}I}$) were uniformly CD44^{hi} and CD62L^{lo} and expressed the proliferation marker Ki67 and high levels of the activation markers and inhibitory receptors PD1 and LAG3 (Figure 1G, top). However, D8 TCR$_{SV40\text{-}I}$ produced only minimal amounts of the pro-inflammatory cytokines interferon (IFN)-γ and tumor necrosis factor (TNF)-α upon ex vivo peptide stimulation (Figure 1G), especially as compared to D8 TCR$_{SV40\text{-}I}$ effectors from normal immunized mice (Figure 1D). This state of hypo-responsiveness became more profound over time (~30 days; D30 TCR$_{SV40\text{-}I}$) with (1) loss of Ki67 positivity, (2) high expression of multiple inhibitory receptors PD1, LAG3, 2B4, and TIM3, and (3) complete failure to produce effector cytokines in response to antigen (Figure 1G, bottom). Dysfunctional T cells did not produce increased levels of the immune-suppressive cytokine IL-10 (Figure S1C), suggesting that tumor-specific CD8$^+$ T cell dysfunction initiated early during tumorigenesis does not reflect conversion to a regulatory CD8$^+$ T cell phenotype (Endharti et al., 2005). The early, dysfunctional state of TCR$_{SV40\text{-}I}$ T cells was further evidenced by failure to control tumor growth or improve survival (Figure S1B).

These phenotypic and functional features of unresponsiveness were previously observed in T cells isolated from solid, late-stage tumors and/or metastases in cancer patients (Gros et al., 2014; Crespo et al., 2013; Zippelius et al., 2004). Thus, T cell differentiation to the dysfunctional state can begin very early during tumor development.

Tumor-Specific T Cells Ultimately Enter a Fixed State of Dysfunction

To determine whether the dysfunctional state of tumor-specific T cells in pre-malignant lesions is reversible, D8 and D30 $TCR_{SV40\text{-}I}$ were re-isolated from livers of ASTxCre-ER^{T2} mice and transferred into antigen-free wild-type (WT) B6 hosts. One day later or at 3–4 weeks after transfer, these secondary recipients were immunized with LM-Tag-I (Figure 2A). Whereas D8 $TCR_{SV40\text{-}I}$ in new hosts were able to proliferate in response to LM-Tag-I and differentiated and acquired phenotypic and functional characteristics of memory $CD8^+$ T cells 1 month after immunization (Figures 2B and 2C), D30 $TCR_{SV40\text{-}I}$ remained unresponsive, failing to proliferate after immunization, even after 3–4 weeks of "parking" in antigen-free hosts (Figures 2B and 2D).

Previous studies have demonstrated that blocking inhibitory receptors (checkpoint blockade) can mediate functional rescue of unresponsive T cells in chronic infection or tumors (Barber et al., 2006; Brahmer et al., 2012; Perez-Gracia et al., 2014; Topalian et al., 2012). Thus, we examined whether PD-1 blockade in vitro could reverse the dysfunctional state of $TCR_{SV40\text{-}I}$ T cells. D8 and D35 $TCR_{SV40\text{-}I}$ were isolated from pre- and early malignant lesions and cultured for 3–4 days in vitro with IL-2 in the absence or presence of PD1 blocking antibody. Although D8 $TCR_{SV40\text{-}I}$ were able to restore effector functions in vitro even in the absence of PD1 blockade, D35 $TCR_{SV40\text{-}I}$ could not be rescued by blockade of the PD1 pathway (Figure 2E). Thus, T cell dysfunction in pre-malignant lesions is progressive and associated with changes in the requirements for T cell rescue: whereas dysfunctional D8 $TCR_{SV40\text{-}I}$ initially appear to be in a plastic cell state and can be re-programmed and rescued to differentiate into functional effector and memory T cells when placed into an antigen-free environment, D30+ dysfunctional $TCR_{SV40\text{-}I}$ ultimately enter a fixed state of dysfunction that persists in the absence of antigen and outside the context of a developing tumor, as well as after PD1 checkpoint blockade in vitro. We next performed in vivo PD1 blockade experiments to better model the rescue strategies being pursued clinically (Figure 2F, top) and found that blockade beginning at D35+ after tumor initiation failed to restore effector functions of D35+ $TCR_{SV40\text{-}I}$. PD1 and PD-L1 blockade did have biologic activity in vivo, resulting in a significant increase in TBET and Ki67 expression (and decrease in PD1 expression), but no increase in expression of the effector molecule Granzyme B or effector cytokines IFN-γ and TNF-α (Figure 2F). In vivo PD1 and PD-L1 blockade starting at D8 after tumor initiation resulted in a significant increase in Granzyme B expression (in addition to an increase in T-bet expression), but still did not rescue cytokine production (Figure S2). The failure of PD1 blockade to fully restore effector functions of D8 and D35+ $TCR_{SV40\text{-}I}$ cells is not totally surprising given the unchanged high expression of numerous other inhibitory receptors such as TIM3, LAG3, and 2B4 after checkpoint blockade (Figures 2F and S2).

Dynamic Molecular Program Associated with the Differentiation and Fate Commitment of Tumor Antigen-Specific T Cells to the Dysfunctional State

The pathways that underlie differentiation of naive, tumor-specific T cells to the dysfunctional state in these early malignant lesions are not known. To identify these molecular programs, we performed comparative whole-genome transcriptome analyses of D8–12 and D34 $TCR_{SV40\text{-}I}$ from pre- and early malignant lesions, as well as from naive (N)

and functional D8-Effector (D8 Eff) $TCR_{SV40\text{-}I}$ after recombinant *Listeria* infection. Notably, D8–12 $TCR_{SV40\text{-}I}$ did not cluster with D8 Eff $TCR_{SV40\text{-}I}$ by principal component analysis (Figure 3A), demonstrating that T cells first encountering antigen in pre- and early malignant lesions did not differentiate through the typical "effector" stage entered by T cells during an acute infection, in which antigen is presented in an inflammatory context and cleared by days 4–5 after infection (Kaech and Cui, 2012). Moreover, D8–12 $TCR_{SV40\text{-}I}$ had a gene signature markedly distinct from D34 $TCR_{SV40\text{-}I}$. Thus, the molecular program induced in D8–12 $TCR_{SV40\text{-}I}$ further evolved with continued antigen exposure, resulting in a "D34-specific" gene signature (Figures 3A and 3B). Both D8–12 and D34 $TCR_{SV40\text{-}I}$ exhibited low expression of effector function genes and transcription factors (e.g., *Tbx21*, *Eomes*, *Id2*, *Gzmk*, *Gzmm*, *Ccr5*, *Cxcr3*) (Figure 3C), consistent with the early inability to produce effector cytokines (Figure 1G) and control tumor outgrowth (Figure S2). K-means analysis revealed that several gene clusters and pathways exhibited progressive up-or downregulation over time (Figures 3C and S3; Table S1): genes controlling T cell function became downregulated from D8–12 to D34, including transcription factors (*Foxo1*, *Foxp1*, *Tcf7*, *Klf2*), signaling molecules (*Lat*, *Jak1*, *Itk*), and chemokine and cytokine receptors (*Ccr7*, *Il7r*), whereas genes associated with reduced immune function became progressively upregulated such as master transcriptional repressors *Egr1*, *Batf* (Kurachi et al., 2014), *Blimp* (Shin et al., 2009), inhibitory receptors *Pdcd1*, *Cd244*, *Cd160*, *Lag3*, and *Ctla4* (Blackburn et al., 2009), and phosphatases *Ptpn11*, *Ptpn12*, *Dusp1*, and *Dusp6* (Figures 3C and S3B). To understand the molecular basis for the transition from a reversible to fixed state of dysfunction, we focused on clusters 5 and 10, whose genes were selectively upregulated in D8–12 $TCR_{SV40\text{-}I}$ (Figures 3C and 3D): in addition to transcription factors *E2f1*, *E2f2*, and *Egr2*, genes controlling nucleosome and chromatin assembly and DNA conformation were highly represented, including histones, mini-chromosome maintenance complex proteins, DNA and histone modifying enzymes (*Dnmt1*, *Dnmt3b*, *Hat*), and the Polycomb-group family member *Ezh2*, a key regulator of repressive chromatin states and transcriptional quiescence (Figures 3C, 3D, and S3C; Viré et al., 2006). Thus, the machinery necessary for epigenetic modification and induction of a repressive chromatin state appear to be expressed early (~D8–12) in tumor-specific T cells (but not in functional D8 Eff) as a result of tumor antigen encounter in pre- and early malignant lesions. This machinery may then establish and ultimately "imprint" an irreversible state of functional unresponsiveness (~D34). These results provide a molecular framework for the early induction and establishment of tumor-specific T cell dysfunction in pre- and early malignant lesions, demonstrating that differentiation to the dysfunctional state is driven by a dynamic gene expression program. This program is notable for alterations of genes in the PI3K/AKT/mTOR, KLF2/EOMES/TBET, FOXO, and JAK-STAT signaling pathways that have been demonstrated to be key determinants of effector and memory T cell differentiation and homeostasis (Kaech and Cui, 2012).

Tumor-Specific $CD8^+$ T Cells Isolated from Pre- and Early Malignant Lesions Exhibit the Molecular Hallmarks of $CD8^+$ T Cells from Late-Stage Human and Mouse Tumors

Because T cells from pre-malignant lesions displayed phenotypic and functional characteristics of dysfunctional T cells from late-stage established tumors from mouse and human (Crespo et al., 2013; Gros et al., 2014; Zippelius et al., 2004), we examined whether

the molecular program of dysfunction initiated in pre-malignant lesions also revealed similarities to that of T cells from late-stage solid tumors. We therefore compared the gene signature of D8 and D34 $TCR_{SV40\text{-}I}$ with that of T cells from late-stage human tumors using the transcriptional profiles of tumor-reactive human Mart-1/Melan-A-specific $CD8^+$ T cells isolated from metastases of melanoma patients (Figures 4A, top, and S4; Baitsch et al., 2011) and $CD8^+$ T cells isolated from established murine melanomas (Figures 4A, bottom, and S4; Giordano et al., 2015), respectively. Gene set enrichment analysis (GSEA) revealed that genes and pathways found to be dysregulated in human, dysfunctional $CD8^+$ T cells from late-stage tumors were enriched in D8 and D34 $TCR_{SV40\text{-}I}$ from pre-malignant lesions, including genes such as *Blimp1*, *Batf*, *Tcf7*, *Foxp1*, *Lef1*, *Bach2*, *Pd1*, *Fasl*, *Cd137*, *Lag3*, *Ctla4*, *Ptpn22*, *Tim3*, and *Dusp1* (Figures 4B and S4). Thus, the phenotypic, functional, and molecular hallmarks of T cell dysfunction described for T cells in late-stage solid human tumors are not necessarily acquired late during tumor development but may rather be "imprinted" at the pre-malignant phase of tumor development.

Tumor-Specific $CD8^+$ T Cells in Pre-malignant Lesions Reveal Conserved and Distinct Molecular Characteristics of Exhausted and Self-Tolerant $CD8^+$ T Cells

"Exhaustion," a state of functional hyporesponsiveness of T cells during chronic infections, arises when pathogens are not quickly eliminated but rather persist, such as in lymphocytic choriomeningitis virus (LCMV) clone 13 infection in mice (Wherry et al., 2007) or human immunodeficiency virus (HIV) infection in humans (Quigley et al., 2010; Schietinger and Greenberg, 2014). It has been suggested that T cells in the context of established, solid human and mouse tumors exhibit an "exhausted" state similar to chronic infections (Baitsch et al., 2011; Giordano et al., 2015) due to high antigen load and the immunosuppressive factors in the microenvironment. We compared the transcriptional profile of D8 $TCR_{SV40\text{-}I}$ from pre-malignant lesions with D8 exhausted virus-specific $CD8^+$ T cells in chronic LCMV (clone 13) infection (Figures 5A and S5; Wherry et al., 2007), as well as ~D30 $TCR_{SV40\text{-}I}$ with ~D30 exhausted virus-specific T cells (Figure 5B and Table S2) using previously identified gene sets of T cell exhaustion. We found an enrichment of exhaustion genes and pathways in $TCR_{SV40\text{-}I}$ from pre-malignant lesions, including *Blimp1*, *Egr2*, *Tcf7*, *Tbx21*, *Jak1*, *Lck*, *Lag3*, *Ctla4*, *Cd244*, and *Pdcd1*. The similarity in the molecular program of dysfunctional T cells encountering a tumor-specific neoantigen in non-inflammatory, pre-malignant lesions with that induced in T cells during chronic viral infection, in which inflammation is present, suggests that induction and establishment of T cell unresponsiveness is primarily driven by antigen chronicity and duration of TCR stimulation rather than environmental signals. However, in addition to the genes and pathways that were conserved, there was a unique signature associated with each setting (Figure 5B and Table S2) and some very distinct differences in the differentiation program. T cell exhaustion during chronic viral infection was previously shown to be associated with progressive differentiation and loss of $TBET^{hi}PD1^{int}$ progenitor T cells and accumulation of terminally differentiated, exhausted $EOMES^{hi}PD1^{hi}GZMB^{hi}$ T cells over the course of infection (Paley et al., 2012). In contrast, dysfunctional tumor-specific T cells did not differentiate into $EOMES^{hi}$ cells but rather lost EOMES expression over the course of tumor progression (Figures 5B, 5C, and S5C) and did not reveal differential GZMB, PD1, and LAG3 expression based on their relative EOMES expression levels (Figure S5C). Thus, T cell

differentiation to the dysfunctional state in tumors is a distinct process from T cell exhaustion during chronic infection. We hypothesize that unresponsive T cells in pre-malignant lesions and chronic viral infections share a conserved program that is driven by persistent antigen independent of context, while also enriching unique genes and pathways that are induced by disparate context-specific, external signals.

Early during the course of chronic viral infections, naive virus-specific T cells initially expand and acquire some effector functions, but as the infection progresses and antigen persists, gradually lose effector functions and differentiate to the exhausted state. In contrast, tumor-specific T cells from pre-malignant lesions do not acquire effector functions, though they do initially proliferate (Figure 1G). Unlike in chronic viral infection, tumor-specific T cells in pre-malignant liver lesions encounter tumor antigen on non-professional and/or non-activated APCs, including transformed hepatocytes, in a non-inflammatory context, a scenario similar to T cells encountering self-antigen in the periphery that also leads to differentiation to an unresponsive state, known as peripheral self-tolerance (Schietinger et al., 2012). Thus, we asked whether the molecular program underlying differentiation of tumor-specific T cells encountering a neo-antigen on transformed cells in pre-malignant lesions is similar to that described for peripheral, self-tolerant T cells encountering self-antigen on normal cells (Schietinger et al., 2012). Cross-tabulation analysis of the gene expression profiles of tumor-specific and self-tolerant T cells revealed several genes and pathways that were similarly dysregulated in both tumor-specific and self-tolerant T cells, including transcription factors *Tbx21*, *Eomes*, *Egr1*, and *Egr2* and inhibitory molecule *CD160* (Figure S6 and Table S3). Genes encoding transcription factors *E2f1* and *E2f2*, inhibitory molecule *Lag3*, and genes associated with epigenetic remodeling, regulation of DNA modification, and chromatin organization, which we previously identified as “self-tolerance-associated” genes (clusters 9 and 13) (Schietinger et al., 2012), were also significantly over-represented in clusters 5 and 10 of $TCR_{SV40\text{-}I}$ which included the early, D8-dysregulated genes described above (Figures 3C and Table S3). However, we also identified many genes and pathways that were uniquely dysregulated in tumor-specific T cells, including the transcription factors *Foxo1*, *Tcf7*, *Foxp1*, *Blimp1*, and *Batf* and inhibitory receptors *Pdcd1*, *Cd244*, *2B4*, *Tim3* (Figures 3C). Thus, context-specific signals that operate in pre-malignant liver lesions comprised of transformed hepatocytes appear to have distinct consequences on the differentiation program and fate of T cells encountering antigen, compared to normal hepatocytes (Comerford et al., 2012).

Presence and Persistence of Antigen Dictates Tumor-Specific $CD8^+$ T Cell Dysfunction in Solid Tumors

To elucidate whether tumor antigen exposure or factors present in the immunosuppressive microenvironment (including immune-suppressive cells, hypoxia, and/or low nutrient levels) drive T cell dysfunction in tumors, we developed a co-transfer model that would allow us to follow the fate of tumor-specific as well as non-tumor-specific T cells within the same immunosuppressive microenvironment of late-stage Tag-expressing solid liver tumors (Figure 6A). 6- to 8-week-old ASTxAlb:Cre (Thy1.2) mice, which constitutively express Cre-recombinase in hepatocytes under the albumin promoter and develop liver tumors upon birth, were used as tumor-bearing hosts (Figure 6B). $TCR_{OT\text{-}I}$ (Ly5.1) $CD8^+$ T cells, which

express a K^b-restricted TCR specific for oval-bumin (OVA), were used as non-tumor-specific T cells (Figure 6A). Naive, tumor-specific $TCR_{SV40\text{-}I}$ were co-transferred with equal numbers of $TCR_{OT\text{-}I}$ into tumor-bearing ASTxAlb:Cre mice or B6 control mice. At 1 day after transfer, host mice were immunized with recombinant *Listeria* co-expressing the Tag-I and OVA epitopes (LM-Tag-I-OVA). $TCR_{SV40\text{-}I}$ and $TCR_{OT\text{-}I}$ expanded equally well in response to LM-Tag-I-OVA, and 7 days after infection similar numbers were found in spleens of control B6 mice (Figure 6C, top). In ASTxAlb:Cre mice, $TCR_{SV40\text{-}I}$ and $TCR_{OT\text{-}I}$ both localized to the tumor-containing livers and were found in equal numbers (Figure 6C, bottom). In B6 hosts, both $TCR_{SV40\text{-}I}$ and $TCR_{OT\text{-}I}$ differentiated into phenotypically and functionally similar effector and memory T cells, typical for T cells during an acute infection in which antigen is being expressed in an inflammatory context and quickly cleared (Figures 6D and 6E). However, in ASTxAlb:Cre mice, $TCR_{SV40\text{-}I}$ and $TCR_{OT\text{-}I}$ entered very distinct differentiation states: tumor-infiltrating, tumor-specific $TCR_{SV40\text{-}I}$ became increasingly dysfunctional with time, expressing high levels of PD1, LAG3, 2B4, and TIM3 and failing to produce effector cytokines in response to cognate antigen similar to T cells in pre-malignant lesions (Figures 6D and 6E). In stark contrast, non-tumor-specific $TCR_{OT\text{-}I}$ isolated from the same tumor site did not upregulate inhibitory receptors (Figure 6D), produced IFN-γ and TNF-α in response to cognate antigen (Figure 6E), and entered a memory differentiation state similar to $TCR_{OT\text{-}I}$ in B6 hosts (Figures 6D and 6E) Thus, tumor-induced T cell dysfunction is driven by the presence and persistence of tumor antigen, and although microenvironmental factors may contribute, they are not sufficient to induce dysfunction. Although many cancer immunotherapies aim to reverse global immunosuppression by modulating the tumor microenvironment, our data suggest that a fundamental level of antigen-specific, cell-intrinsic dysfunction must also be overcome.

DISCUSSION

In summary, by following the fate of naive, tumor-specific $CD8^+$ T cells after tumor initiation, we uncovered the mechanistic underpinnings of T cell differentiation and dysfunction in solid tumors. The differentiation of naive, tumor-specific T cells begins early during tumor development in a dynamic process that ultimately results in the establishment of a fixed state of dysfunction, even before the emergence of a pathologically defined malignant tumor. We found that $TCR_{SV40\text{-}I}$ from pre-malignant lesions harbored many of the same phenotypic, functional, and molecular hallmarks described for human T cells in late-stage solid tumors and/or metastases suggesting that such hallmarks are already “imprinted” at the pre- and early malignant phase. Furthermore, fate commitment to the dysfunctional state requires continuous tumor antigen encounter and TCR stimulation, and, though microenvironmental factors may play a role, they are not sufficient to induce the dysfunctional phenotype.

$CD8^+$ T cell differentiation is tightly controlled and dependent on the nature, context, and duration of antigen encounter. When naive $CD8^+$ T cells encounter (foreign) antigen in a stimulatory, inflammatory context (e.g., acute infection), a cell-intrinsic activation and differentiation program is initiated, driving T cells to expand and differentiate into cytolytic effector cells that control and eventually clear the pathogen and antigen (expansion phase). After antigen clearance (approximately 5–6 days after infection), most effector T cells

undergo apoptosis (contraction phase), with some T cells surviving and differentiating into memory T cells (memory phase). Each differentiation state—naive, effector, and memory—has a unique transcriptional program that defines the phenotypic and functional characteristics (Kaech and Cui, 2012). Changes in the context and duration of antigen encounter can cause alterations in this differentiation process: if antigen is presented on non-professional, non-activated APC in a non-inflammatory context, and/or if antigen persists, naive T cells are unable to differentiate to the memory state but instead enter a differentiation program associated with functional unresponsiveness. Such differentiation states include anergy, exhaustion in chronic infections, and self-tolerance (Schietinger and Greenberg, 2014). Here we demonstrate that T cell dysfunction against tumor-specific neoantigens represents a distinct differentiation state that is initiated after antigen encounter in a non-inflammatory context (on non-professional and/or non-activated APCs) and "imprinted" through a cell-intrinsic dynamic program driven by continuous antigen exposure. The failure to acquire effector functions probably reflects in part characteristics of the interaction with hepatocytes as APCs. Hepatocytes do not express the co-stimulatory molecules CD80 or CD86 that deliver signals to T cells via CD28. CD28 is a major co-stimulatory molecule required for the induction of effector T cell function and synthesis of cytokines, and T cells primed in the absence of CD28-mediated signals have been shown to enter an unresponsive state (anergy). Indeed, $TCR_{SV40\text{-}I}$ from pre- and early malignant lesions do not express CD28, in contrast to effector T cells during *Listeria* infections (Figure S3B), which encounter antigen in an inflammatory context on professional activated APCs that express high levels of CD80 and CD86 (Mittrücker et al., 2001).

Studies of acute and chronic viral infections demonstrate that differentiation of naive virus-specific $CD8^+$ T cells toward a functional memory (acute infection) or dysfunctional exhaustion state (chronic infection) is epigenetically and transcriptionally induced with remarkably early kinetics (~5–8 days after infection) (Young-blood et al., 2011). Similarly, tumor-specific T cell dysfunction is initiated early after tumor initiation and antigen encounter (by ~D8) and evolves with continued antigen exposure. Moreover, there was substantial similarity in the molecular programs of unresponsive tumor-specific $TCR_{SV40\text{-}I}$ T cells and exhausted T cells during chronic viral infection (Figure 5). The fact that (1) disparate settings of continued antigen presentation—non-inflammatory (pre-malignant lesions) and highly inflammatory (chronic viral infection)—induce closely related phenotypic, functional, and molecular programs of dysfunction and (2) non-tumor antigen-specific $TCR_{OT\text{-}I}$ T cells remain functional in the immunosuppressive environment of late-stage solid tumors, suggests that persistence of tumor antigen, rather than microenvironmental factors, is required for the differentiation to the dysfunctional state. This does not preclude a role for the microenvironment and context, because chronic antigen with persistent TCR stimulation may induce tumor-specific T cell dysfunction in part by mediating the upregulation of inhibitory receptors (e.g., PD1) and thereby increasing the susceptibility of tumor-specific T cells to inhibitory signals from the environment (e.g., inhibitory receptor ligands such as PD-L1 or PD-L2).

In addition to the molecular and phenotypic similarities between dysfunctional tumor-specific and exhausted virus-specific T cells, there was a unique signature and phenotype for each setting, suggesting that T cell differentiation to the dysfunctional state in tumors is a

distinct process from T cell exhaustion during chronic infection. We hypothesize that genes and pathways conserved in different settings of T cell dysfunction reflect a core program of dysfunction driven by persistent antigen, whereas genes and pathways unique for each setting probably reflect disparate, context- and environment-specific, external signals (Figure S7 and Table S4).

When tumor-specific $TCR_{SV40\text{-}I}$ were removed by D8 from persistent tumor antigen and pre-malignant lesion and provided with optimal activation signals in an appropriate (acute) context, differentiation to the dysfunctional state was aborted and T cells were able to differentiate to functional memory T cells, in contrast to later stage dysfunctional (D34) $TCR_{SV40\text{-}I}$, which could not be rescued by antigen withdrawal or checkpoint blockade (Figure 2). Thus, although early dysfunction is still a plastic differentiation state, it ultimately becomes fixed and non-rescuable by antigen withdrawal and/or PD1 and PD-L1 checkpoint blockade. Several recent clinical studies now demonstrate that T cells that recognize tumor-specific mutant antigens can be functionally rescued by checkpoint blockade (PD1, PD-L1, CTLA4) or expansion in vitro (Gubin et al., 2014; Lu et al., 2013; Rizvi et al., 2015; Robbins et al., 2013; Snyder et al., 2014; Tran et al., 2014; van Rooij et al., 2013; Wolchok and Chan, 2014). However, those T cells have not been found to recognize oncogenic driver antigens, but rather see epitopes from mutant proteins not previously associated with tumorigenesis. Although the inability to detect driver antigen-specific T cells with restored effector functions after checkpoint blockade may reflect lack of creation of immunogenic epitopes in some settings (e.g., mutant KRAS), our data suggest that even when the oncogenic driver contains potentially immunogenic epitopes, driver-specific T cells may be not rescuable because of the establishment of an imprinted state of dysfunction early during tumorigenesis. It is tempting to speculate that differences may exist between the cell-intrinsic differentiation programs and consequently requirements for functional rescue of T cells specific for mutant driver antigens and T cells specific for mutational antigens that arise later during tumor development, e.g., when genomic instability in cancer cells leads to the creation of additional mutations and antigens (passenger mutations).

Which immunomodulatory strategies or genes must be targeted to achieve functional rescue of tumor-specific T cells, including T cells specific for oncogenic driver antigens, remains to be determined; several inhibitory receptors including PD1, LAG3, 2B4, TIM3, CTLA4, and CD160 were found to be overexpressed (Figures 1G and 3C), and thus combinational therapeutic approaches could have the potential to reverse T cell dysfunction, e.g., by checkpoint blockade targeting multiple inhibitory receptors in combination with activation and proliferation signals (Schietinger and Greenberg, 2014). Because anti-tumor T cell responses are potentially impacted by factors such as (1) antigen expression level (Philip et al., 2010) and processing (Popovic et al., 2011), (2) affinity and ability to form class I binding epitopes (Khalili et al., 2012), (3) tissue-of-origin, (4) presence of anatomical and/or tumor microenvironmental barriers that sequester antigen from immune surveillance (T cell exclusion, immune privilege) (Hamzah et al., 2008; Joyce and Fearon, 2015), and/or (5) the presence of tumor-specific $CD4^+$ T cells, multiple factors will likely determine the differentiation state of dysfunctional tumor-specific T cells and ultimately the success or failure of immunotherapeutic approaches. Elucidating the molecular mechanisms that

establish and maintain antigen-driven, dysfunctional differentiation of tumor-specific T cells has the potential to lead to new effective immunotherapeutic interventions.

EXPERIMENTAL PROCEDURES

Mice

AST (Albumin-floxStop-SV40 large T antigen [Tag]) mice were provided by N.G. and G.J.H. from the German Cancer Research Center (Stahl et al., 2009). $TCR_{SV40\text{-}I}$ transgenic (B6.Cg-Tg(TcraY1,TcrbY1)416Tev/J) (Staveley-O'Carroll et al., 2003), Cre-ER^{T2} (B6.129-*Gt(ROSA)26Sor*$^{tm1(cre/ERT2)Tyj}$/ J), Alb:Cre (B6.Cg-Tg(Alb-cre)21Mgn/J), C57BL/6J Thy1.2, and Thy1.1 (B6.PL-*Thy1*^{a}/CyJ) mice were purchased from The Jackson Laboratory. $TCR_{SV40\text{-}I}$ mice were crossed to Thy.1.1 mice in our animal facility to generate $TCR_{SV40\text{-}I}$ Thy.1.1 mice. AST mice were crossed to Cre-ER^{T2} or Alb:Cre mice to obtain ASTxCre-ER^{T2} and ASTxAlb:Cre mice, respectively. OT-I TCR transgenic mice (Hogquist et al., 1994) were a gift from M. Bevan (University of Washington). Ly5.1 mice were purchased from The Jackson Laboratory. OT-I TCR transgenic mice were crossed to Ly5.1 mice to generate OT-I Ly5.1 mice. All mice were bred and maintained in a specific-pathogen-free barrier facility at the University of Washington and in the animal facility at Memorial Sloan Kettering Cancer Center. Experiments were performed in compliance with the University of Washington and Memorial Sloan Kettering Cancer Center Institutional Animal Care and Use Committee regulations.

Antibodies and Reagents

The SV40 large T antigen epitope I (Tag-I) peptide (SAINNYAQKL) was purchased from Pi Proteomics. The H-2D^{b}/Tag-I tetramer was synthesized by the Immune Monitoring Core at the Fred Hutchinson Cancer Research Center. The fluorochrome-conjugated antibodies were purchased from BD Biosciences, eBioscience, and Biolegend. Tamoxifen was purchased from Sigma-Aldrich. For tamoxifen induction, a tamoxifen stock solution (5 mg/mL in corn oil) was prepared by warming tamoxifen in 1 mL sterile corn oil at 65°C for about 15 min, then further diluted in corn oil to obtain the stock concentration of 5 mg/mL. 1 mg tamoxifen (= 200 μL) was administered once intraperitoneally (i.p.) into ASTxCre-ER^{T2} mice.

Listeria Infection

The *Listeria monocytogenes* (Lm) Δ*actA* Δ*inlB* strain (Brockstedt et al., 2004) expressing the Tag-I epitope (SAINNYAQKL, SV40 large T $antigen_{206\text{-}215}$) together with OT-I epitope (SIINFEKL, $OVA_{257\text{-}264}$) was generated by Aduro BioTech. Lm strain was constructed using the previously described strategy (Sinnathamby et al., 2009). Experimental vaccination stocks were prepared by growing bacteria to early stationary phase, washing in phosphate buffered saline, formulated at approximately 1×10^{10} colony forming units (cfu)/mL, and stored at −80°C. Mice were infected i.p. with 5×10^{6} cfu of LM-Tag-I (also called LM-Tag-I-OVA in Figure 6).

Adoptive T Cell Transfers

Naive $CD8^+$ splenocytes from $TCR_{SV40\text{-}I}$ Thy1.1 transgenic mice were adoptively transferred into ASTxCre-ER^{T2} mice; 1–2 days later, mice were treated with 1 mg tamoxifen. For $TCR_{SV40\text{-}I}$ and $TCR_{OT\text{-}I}$ co-transfer experiments in Figure 6, 3–4 × 10^4 $TCR_{SV40\text{-}I}$ Thy1.1 and $TCR_{OT\text{-}I}$ Ly5.1 $CD8^+$ T cells were adoptively transferred into ASTxAlb:Cre mice or B6 control mice; 1 day later, mice were infected with 5 × 10^6 cfu LM-Tag-I-OVA (co-expressing the OVA epitope SIINFEKL). For the generation of effector and memory $TCR_{SV40\text{-}I}$ $CD8^+$ T cells, naive $CD8^+$ splenocytes from $TCR_{SV40\text{-}I}$ Thy1.1 transgenic mice were adoptively transferred into B6 (Thy1.2) mice; 1 day later, mice were infected with 5 × 10^6 cfu LM-Tag-I. Effector $TCR_{SV40\text{-}I}$ $CD8^+$ T cells were isolated from the spleens of B6 host mice and analyzed 8 days after *Listeria* infection; memory $TCR_{SV40\text{-}I}$ $CD8^+$ T cells were isolated from spleens of B6 host mice and analyzed at least 2–3 months after *Listeria* infection.

Supplementary Material

Refer to Web version on PubMed Central for supplementary material.

Acknowledgments

We thank X. Tan, S. Funk, and I. Roberts for technical support, C. Chou and the other members of the Greenberg lab and the Program of Immunology (FHCRC) for helpful discussions, M. Black from the UW Flow Cytometry Core lab, J. Cao from the Immune Monitoring, C. Bennett from the Genomics Shared Resource (FHCRC), the MSKCC Flow Cytometry Core facility; and Bill Hanson from Aduro BioTech for technical help with the construction of the *Listeria* strains. This work was supported by the Irvington Institute Fellowship Program of the Cancer Research Institute (to A.S.), NIH/NCI grant K99/R00 CA172371 (to A.S.), the V Foundation for Cancer Research (to A.S.), the Josie Robertson Young Investigators Program (to A.S.), the MSK Cancer Center Support Grant/ Core Grant P30 CA008748; R01 CA033084, R21 AI107776 (to P.D.G.), grant FND 7008-08 from the Korean Research Institute of Bioscience and Biotechnology (to P.D.G.), NIH grant P30 CA015704-39 (J.J.D. and R.S.B.), and NIH grant K08CA158069 (to M.P.). N.G. is a member of the DFG Cluster of Excellence Immunosensation.

References

Alexandrov LB, Nik-Zainal S, Wedge DC, Aparicio SA, Behjati S, Biankin AV, Bignell GR, Bolli N, Borg A, Børresen-Dale AL, et al. Signatures of mutational processes in human cancer. Nature. 2013; 500:415–421. [PubMed: 23945592]

Baitsch L, Baumgaertner P, Devêvre E, Raghav SK, Legat A, Barba L, Wieckowski S, Bouzourene H, Deplancke B, Romero P, et al. Exhaustion of tumor-specific $CD8^+$ T cells in metastases from melanoma patients. J Clin Invest. 2011; 121:2350–2360. [PubMed: 21555851]

Barber DL, Wherry EJ, Masopust D, Zhu B, Allison JP, Sharpe AH, Freeman GJ, Ahmed R. Restoring function in exhausted CD8 T cells during chronic viral infection. Nature. 2006; 439:682–687. [PubMed: 16382236]

Blackburn SD, Shin H, Haining WN, Zou T, Workman CJ, Polley A, Betts MR, Freeman GJ, Vignali DA, Wherry EJ. Coregulation of CD8+ T cell exhaustion by multiple inhibitory receptors during chronic viral infection. Nat Immunol. 2009; 10:29–37. [PubMed: 19043418]

Brahmer JR, Tykodi SS, Chow LQ, Hwu WJ, Topalian SL, Hwu P, Drake CG, Camacho LH, Kauh J, Odunsi K, et al. Safety and activity of anti-PD-L1 antibody in patients with advanced cancer. N Engl J Med. 2012; 366:2455–2465. [PubMed: 22658128]

Brockstedt DG, Giedlin MA, Leong ML, Bahjat KS, Gao Y, Luckett W, Liu W, Cook DN, Portnoy DA, Dubensky TW Jr. Listeria-based cancer vaccines that segregate immunogenicity from toxicity. Proc Natl Acad Sci USA. 2004; 101:13832–13837. [PubMed: 15365184]

Comerford SA, Schultz N, Hinnant EA, Klapproth S, Hammer RE. Comparative analysis of SV40 17kT and LT function in vivo demonstrates that LT's C-terminus re-programs hepatic gene expression and is necessary for tumorigenesis in the liver. Oncogenesis. 2012; 1:e28. [PubMed: 23552841]

Crespo J, Sun H, Welling TH, Tian Z, Zou W. T cell anergy, exhaustion, senescence, and stemness in the tumor microenvironment. Curr Opin Immunol. 2013; 25:214–221. [PubMed: 23298609]

Cui W, Kaech SM. Generation of effector CD8+ T cells and their conversion to memory T cells. Immunol Rev. 2010; 236:151–166. [PubMed: 20636815]

Cullen JM, Sandgren EP, Brinster RL, Maronpot RR. Histologic characterization of hepatic carcinogenesis in transgenic mice expressing SV40 T-antigens. Vet Pathol. 1993; 30:111–118. [PubMed: 8385835]

Endharti AT, Rifa'I M, Shi Z, Fukuoka Y, Nakahara Y, Kawamoto Y, Takeda K, Isobe K, Suzuki H. Cutting edge: CD8+CD122+ regulatory T cells produce IL-10 to suppress IFN-gamma production and proliferation of CD8+ T cells. J Immunol. 2005; 175:7093–7097. [PubMed: 16301610]

Gabrilovich DI, Ostrand-Rosenberg S, Bronte V. Coordinated regulation of myeloid cells by tumours. Nat Rev Immunol. 2012; 12:253–268. [PubMed: 22437938]

Giordano M, Henin C, Maurizio J, Imbratta C, Bourdely P, Buferne M, Baitsch L, Vanhille L, Sieweke MH, Speiser DE, et al. Molecular profiling of CD8 T cells in autochthonous melanoma identifies Maf as driver of exhaustion. EMBO J. 2015; 34:2042–2058. [PubMed: 26139534]

Gros A, Robbins PF, Yao X, Li YF, Turcotte S, Tran E, Wunderlich JR, Mixon A, Farid S, Dudley ME, et al. PD-1 identifies the patient-specific $CD8^{+}$ tumor-reactive repertoire infiltrating human tumors. J Clin Invest. 2014; 124:2246–2259. [PubMed: 24667641]

Gubin MM, Zhang X, Schuster H, Caron E, Ward JP, Noguchi T, Ivanova Y, Hundal J, Arthur CD, Krebber WJ, et al. Checkpoint blockade cancer immunotherapy targets tumour-specific mutant antigens. Nature. 2014; 515:577–581. [PubMed: 25428507]

Hamzah J, Jugold M, Kiessling F, Rigby P, Manzur M, Marti HH, Rabie T, Kaden S, Gröne HJ, Hämmerling GJ, et al. Vascular normalization in Rgs5-deficient tumours promotes immune destruction. Nature. 2008; 453:410–414. [PubMed: 18418378]

Hellström I, Hellström KE, Pierce GE, Yang JP. Cellular and humoral immunity to different types of human neoplasms. Nature. 1968; 220:1352–1354. [PubMed: 4302696]

Hogquist KA, Jameson SC, Heath WR, Howard JL, Bevan MJ, Carbone FR. T cell receptor antagonist peptides induce positive selection. Cell. 1994; 76:17–27. [PubMed: 8287475]

Joyce JA, Fearon DT. T cell exclusion, immune privilege, and the tumor microenvironment. Science. 2015; 348:74–80. [PubMed: 25838376]

Kaech SM, Cui W. Transcriptional control of effector and memory CD8+ T cell differentiation. Nat Rev Immunol. 2012; 12:749–761. [PubMed: 23080391]

Khalili JS, Hanson RW, Szallasi Z. In silico prediction of tumor antigens derived from functional missense mutations of the cancer gene census. OncoImmunology. 2012; 1:1281–1289. [PubMed: 23243591]

Kubuschok B, Neumann F, Breit R, Sester M, Schormann C, Wagner C, Sester U, Hartmann F, Wagner M, Remberger K, et al. Naturally occurring T-cell response against mutated p21 ras oncoprotein in pancreatic cancer. Clin Cancer Res. 2006; 12:1365–1372. [PubMed: 16489095]

Kurachi M, Barnitz RA, Yosef N, Odorizzi PM, DiIorio MA, Lemieux ME, Yates K, Godec J, Klatt MG, Regev A, et al. The transcription factor BATF operates as an essential differentiation checkpoint in early effector CD8+ T cells. Nat Immunol. 2014; 15:373–383. [PubMed: 24584090]

Lennerz V, Fatho M, Gentilini C, Frye RA, Lifke A, Ferel D, Wölfel C, Huber C, Wölfel T. The response of autologous T cells to a human melanoma is dominated by mutated neoantigens. Proc Natl Acad Sci USA. 2005; 102:16013–16018. [PubMed: 16247014]

Linnemann C, van Buuren MM, Bies L, Verdegaal EM, Schotte R, Calis JJ, Behjati S, Velds A, Hilkmann H, Atmioui DE, et al. High-throughput epitope discovery reveals frequent recognition of neo-antigens by CD4+ T cells in human melanoma. Nat Med. 2015; 21:81–85. [PubMed: 25531942]

Lu YC, Yao X, Li YF, El-Gamil M, Dudley ME, Yang JC, Almeida JR, Douek DC, Samuels Y, Rosenberg SA, Robbins PF. Mutated PPP1R3B is recognized by T cells used to treat a melanoma

patient who experienced a durable complete tumor regression. J Immunol. 2013; 190:6034–6042. [PubMed: 23690473]

Mittrücker HW, Kursar M, Köhler A, Hurwitz R, Kaufmann SH. Role of CD28 for the generation and expansion of antigen-specific CD8(+) T lymphocytes during infection with *Listeria monocytogenes*. J Immunol. 2001; 167:5620–5627. [PubMed: 11698433]

Noy R, Pollard JW. Tumor-associated macrophages: from mechanisms to therapy. Immunity. 2014; 41:49–61. [PubMed: 25035953]

Ostrand-Rosenberg S, Horn LA, Haile ST. The programmed death-1 immune-suppressive pathway: barrier to antitumor immunity. J Immunol. 2014; 193:3835–3841. [PubMed: 25281753]

Paley MA, Kroy DC, Odorizzi PM, Johnnidis JB, Dolfi DV, Barnett BE, Bikoff EK, Robertson EJ, Lauer GM, Reiner SL, Wherry EJ. Progenitor and terminal subsets of CD8+ T cells cooperate to contain chronic viral infection. Science. 2012; 338:1220–1225. [PubMed: 23197535]

Perez-Gracia JL, Labiano S, Rodriguez-Ruiz ME, Sanmamed MF, Melero I. Orchestrating immune check-point blockade for cancer immunotherapy in combinations. Curr Opin Immunol. 2014; 27:89–97. [PubMed: 24485523]

Philip M, Schietinger A, Schreiber H. Ribosomal versus non-ribosomal cellular antigens: factors determining efficiency of indirect presentation to CD4+ T cells. Immunology. 2010; 130:494–503. [PubMed: 20331471]

Popovic J, Li LP, Kloetzel PM, Leisegang M, Uckert W, Blankenstein T. The only proposed T-cell epitope derived from the TEL-AML1 translocation is not naturally processed. Blood. 2011; 118:946–954. [PubMed: 21613253]

Quigley M, Pereyra F, Nilsson B, Porichis F, Fonseca C, Eichbaum Q, Julg B, Jesneck JL, Brosnahan K, Imam S, et al. Transcriptional analysis of HIV-specific CD8+ T cells shows that PD-1 inhibits T cell function by upregulating BATF. Nat Med. 2010; 16:1147–1151. [PubMed: 20890291]

Rizvi NA, Hellmann MD, Snyder A, Kvistborg P, Makarov V, Havel JJ, Lee W, Yuan J, Wong P, Ho TS, et al. Cancer immunology. Mutational landscape determines sensitivity to PD-1 blockade in non-small cell lung cancer. Science. 2015; 348:124–128. [PubMed: 25765070]

Robbins PF, El-Gamil M, Li YF, Kawakami Y, Loftus D, Appella E, Rosenberg SA. A mutated beta-catenin gene encodes a melanoma-specific antigen recognized by tumor infiltrating lymphocytes. J Exp Med. 1996; 183:1185–1192. [PubMed: 8642260]

Robbins PF, Lu YC, El-Gamil M, Li YF, Gross C, Gartner J, Lin JC, Teer JK, Cliften P, Tycksen E, et al. Mining exomic sequencing data to identify mutated antigens recognized by adoptively transferred tumor-reactive T cells. Nat Med. 2013; 19:747–752. [PubMed: 23644516]

Savage PA, Malchow S, Leventhal DS. Basic principles of tumor-associated regulatory T cell biology. Trends Immunol. 2013; 34:33–40. [PubMed: 22999714]

Schietinger A, Greenberg PD. Tolerance and exhaustion: defining mechanisms of T cell dysfunction. Trends Immunol. 2014; 35:51–60. [PubMed: 24210163]

Schietinger A, Philip M, Schreiber H. Specificity in cancer immunotherapy. Semin Immunol. 2008; 20:276–285. [PubMed: 18684640]

Schietinger A, Delrow JJ, Basom RS, Blattman JN, Greenberg PD. Rescued tolerant CD8 T cells are preprogrammed to reestablish the tolerant state. Science. 2012; 335:723–727. [PubMed: 22267581]

Shin H, Blackburn SD, Intlekofer AM, Kao C, Angelosanto JM, Reiner SL, Wherry EJ. A role for the transcriptional repressor Blimp-1 in CD8(+) T cell exhaustion during chronic viral infection. Immunity. 2009; 31:309–320. [PubMed: 19664943]

Sinnathamby G, Lauer P, Zerfass J, Hanson B, Karabudak A, Krakover J, Secord AA, Clay TM, Morse MA, Dubensky TW Jr, et al. Priming and activation of human ovarian and breast cancer-specific CD8+ T cells by polyvalent *Listeria monocytogenes*-based vaccines. J Immunother. 2009; 32:856–869. [PubMed: 19752748]

Snyder A, Makarov V, Merghoub T, Yuan J, Zaretsky JM, Desrichard A, Walsh LA, Postow MA, Wong P, Ho TS, et al. Genetic basis for clinical response to CTLA-4 blockade in melanoma. N Engl J Med. 2014; 371:2189–2199. [PubMed: 25409260]

Stahl S, Sacher T, Bechtold A, Protzer U, Ganss R, Hämmerling GJ, Arnold B, Garbi N. Tumor agonist peptides break tolerance and elicit effective CTL responses in an inducible mouse model of hepatocellular carcinoma. Immunol Lett. 2009; 123:31–37. [PubMed: 19428549]

Staveley-O'Carroll K, Schell TD, Jimenez M, Mylin LM, Tevethia MJ, Schoenberger SP, Tevethia SS. In vivo ligation of CD40 enhances priming against the endogenous tumor antigen and promotes CD8+ T cell effector function in SV40 T antigen transgenic mice. J Immunol. 2003; 171:697–707. [PubMed: 12847236]

Thomas RM, Gao L, Wells AD. Signals from CD28 induce stable epigenetic modification of the IL-2 promoter. J Immunol. 2005; 174:4639–4646. [PubMed: 15814687]

Topalian SL, Hodi FS, Brahmer JR, Gettinger SN, Smith DC, McDermott DF, Powderly JD, Carvajal RD, Sosman JA, Atkins MB, et al. Safety, activity, and immune correlates of anti-PD-1 antibody in cancer. N Engl J Med. 2012; 366:2443–2454. [PubMed: 22658127]

Tran E, Turcotte S, Gros A, Robbins PF, Lu YC, Dudley ME, Wunderlich JR, Somerville RP, Hogan K, Hinrichs CS, et al. Cancer immunotherapy based on mutation-specific CD4+ T cells in a patient with epithelial cancer. Science. 2014; 344:641–645. [PubMed: 24812403]

van Rooij N, van Buuren MM, Philips D, Velds A, Toebes M, Heemskerk B, van Dijk LJ, Behjati S, Hilkmann H, El Atmioui D, et al. Tumor exome analysis reveals neoantigen-specific T-cell reactivity in an ipilimumab-responsive melanoma. J Clin Oncol. 2013; 31:e439–e442. [PubMed: 24043743]

Viré E, Brenner C, Deplus R, Blanchon L, Fraga M, Didelot C, Morey L, Van Eynde A, Bernard D, Vanderwinden JM, et al. The Polycomb group protein EZH2 directly controls DNA methylation. Nature. 2006; 439:871–874. [PubMed: 16357870]

Wherry EJ, Ha SJ, Kaech SM, Haining WN, Sarkar S, Kalia V, Subramaniam S, Blattman JN, Barber DL, Ahmed R. Molecular signature of CD8+ T cell exhaustion during chronic viral infection. Immunity. 2007; 27:670–684. [PubMed: 17950003]

Willimsky G, Blankenstein T. Sporadic immunogenic tumours avoid destruction by inducing T-cell tolerance. Nature. 2005; 437:141–146. [PubMed: 16136144]

Wolchok JD, Chan TA. Cancer: Antitumour immunity gets a boost. Nature. 2014; 515:496–498. [PubMed: 25428495]

Wölfel T, Hauer M, Schneider J, Serrano M, Wölfel C, Klehmann-Hieb E, De Plaen E, Hankeln T, Meyer zum Büschenfelde KH, Beach D. A p16INK4a-insensitive CDK4 mutant targeted by cytolytic T lymphocytes in a human melanoma. Science. 1995; 269:1281–1284. [PubMed: 7652577]

Youngblood B, Oestreich KJ, Ha SJ, Duraiswamy J, Akondy RS, West EE, Wei Z, Lu P, Austin JW, Riley JL, et al. Chronic virus infection enforces demethylation of the locus that encodes PD-1 in antigen-specific CD8(+) T cells. Immunity. 2011; 35:400–412. [PubMed: 21943489]

Zippelius A, Batard P, Rubio-Godoy V, Bioley G, Liénard D, Lejeune F, Rimoldi D, Guillaume P, Meidenbauer N, Mackensen A, et al. Effector function of human tumor-specific CD8 T cells in melanoma lesions: a state of local functional tolerance. Cancer Res. 2004; 64:2865–2873. [PubMed: 15087405]

Highlights

- Tumor-specific T cells become dysfunctional at the pre- and early malignant stage
- T cell dysfunction is initially reversible but later becomes irreversible
- Dysfunctional T cells from pre- and early malignant lesions are similar to tumor-reactive T cells in late human tumors
- Continuous antigen encounter rather than microenvironmental factors drive dysfunction

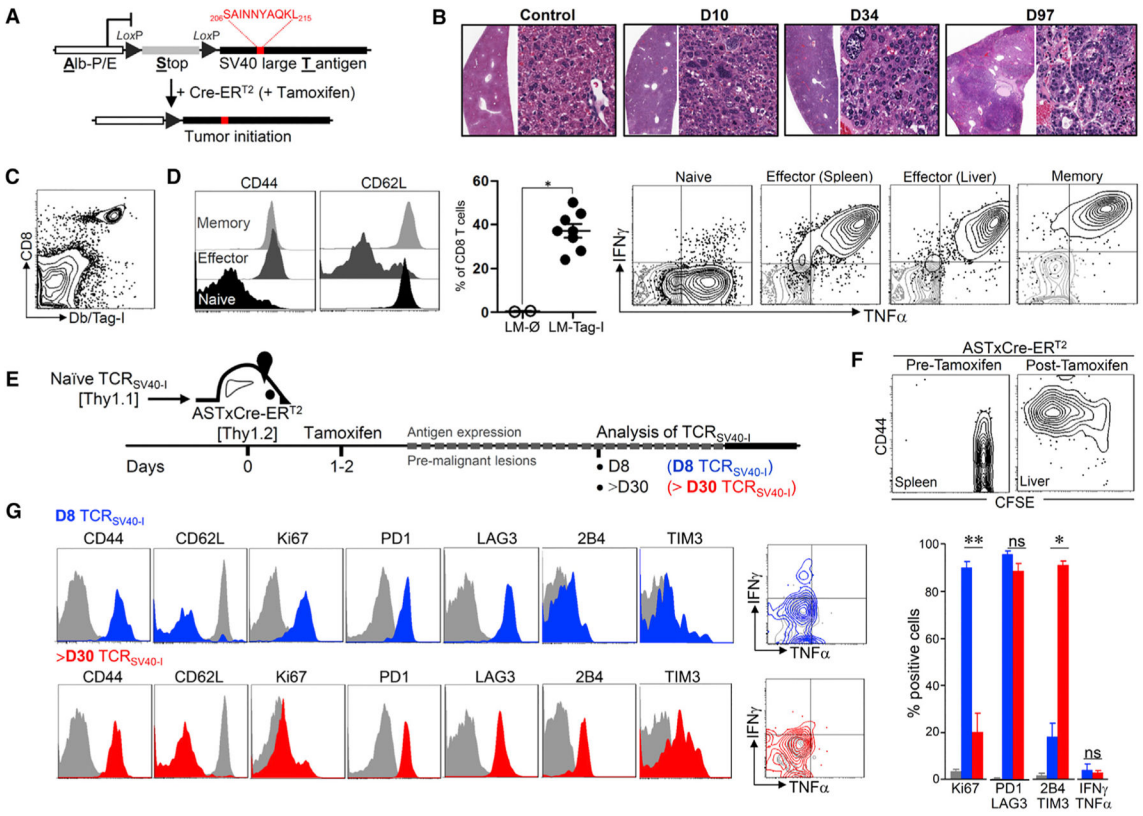

Figure 1. Rapid Induction of Dysfunction in Naive Tumor-Specific CD8$^+$ T Cells Encountering an Oncogenic Driver Neoantigen in Pre-malignant Lesions

(A) Tamoxifen (Tam)-inducible ASTxCre-ER^{T2} tumor model. Tam-induced Cre-mediated excision of the flox-stop cassette leads to SV40 large T antigen expression. Peptide sequence in red indicates epitope I recognized by transgenic TCR$_{SV40\text{-}I}$ CD8$^+$ T cells.

(B) Liver carcinogenesis in ASTxCre-ER^{T2} mice. Hematoxylin and eosin (H&E) staining of liver sections collected at D10, D34, and D97 after Tam treatment. See also Figure S1.

(C) Flow cytometric analysis of CD8$^+$ splenocytes from TCR$_{SV40\text{-}I}$ transgenic mice using Db/Tag-I tetramers.

(D) Differentiation of naive TCR$_{SV40\text{-}I}$ CD8$^+$ T cells into functional effector and memory T cells. Left: Expression levels of CD44 and CD62L. Middle: 1 day after adoptive transfer of naive TCR$_{SV40\text{-}I}$ (Thy1.1$^+$) into B6 (Thy1.2$^+$) hosts, mice were immunized with 5 × 10^6 cfu of LM-Tag-I or control LM-Ø. At 7 days after infection, peripheral blood was analyzed for expansion of donor TCR$_{SV40\text{-}I}$. Each symbol represents an individual mouse; data show mean ± SEM. *$p < 0.0001$. Results are representative of at least ten independent experiments. Right: Intracellular IFN-γ and TNF-α production for naive, effector (8 days after LM-Tag-I), and memory (2–3 months LM-Tag-I) T cells. FACS plots are gated on CD8$^+$Thy1.1$^+$ cells.

(E) Experimental scheme.

(F) CD44 expression and carboxy-fluorescein-succimidyl ester (CFSE) dilution of transferred, naive TCR$_{SV40\text{-}I}$ isolated from spleens of ASTxCre-ER^{T2} 1–2 days after transfer (left) and isolated from livers 3 days after Tam (right).

(G) CD44, CD62L, Ki67, PD1, LAG3, 2B4, and TIM3 expression of D8 $TCR_{SV40\text{-}I}$ (blue) and D30 $TCR_{SV40\text{-}I}$ (red) isolated from livers of Tam-treated ASTxCre-ER^{T2} mice, and intracellular IFN-γ and TNF-α production. Naive T cells are shown as controls (gray). Results are representative of at least six independent experiments; data show mean ± SEM (*p = 0.0001, **p < 0.0001; ns, not statistically significant) using unpaired, two-tailed Student's t test (for analysis between groups ~D8 and >D30 from 2–3 independent experiments).

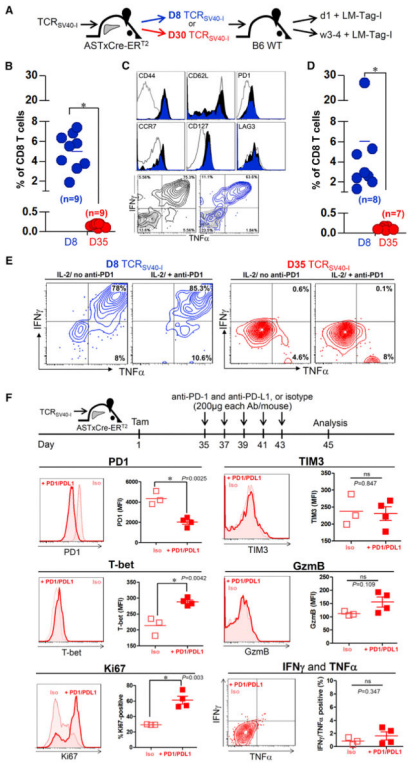

Figure 2. Tumor-Specific CD8$^+$ T Cells in Pre-malignant Lesions Enter a Fixed State of Dysfunction Not Reliant on External Cues

(A) Experimental scheme. D8 and D30 $TCR_{SV40\text{-}I}$ were isolated from livers and transferred into normal B6 mice and immunized with LM-Tag-I either 1 day or 3–4 weeks after transfer.

(B) 1 day after second transfer, mice were immunized with 5×10^6 cfu of LM-Tag-I, and 7 days later, spleens were analyzed for expansion of donor T cells by flow cytometry. *p = 0.00042 using Mann-Whitney U-test.

(C) D8 $TCR_{SV40\text{-}I}$ that expanded after immunization as described in (B) were isolated from spleens 1 month later and evaluated for CD44, CD62L, PD1, LAG3, CCR7, and CD127 expression, and for IFN-γ and TNF-α production in response to antigen ex vivo. D8 $TCR_{SV40\text{-}I}$ (blue); naive (gray) and memory (solid black) are shown as controls.

(D) 3–4 weeks after second transfer mice were immunized and analyzed as described in (B). Each symbol represents an individual mouse with the mean shown. Data are pooled from two independent experiments, with n = 8–9 for D8 $TCR_{SV40\text{-}I}$ and n = 7–9 for D30 $TCR_{SV40\text{-}I}$. *p = 0.0015 using Mann-Whitney U-test.

(E) D8 and D35 $TCR_{SV40\text{-}I}$ were cultured in vitro for 72 hr in the presence of IL-2 with or without anti-PD1 antibody (IL-2 [20 U/mL]; anti-PD1 [10 μg/mL; clone RMP1-14]). IFN-γ and TNF-α production was determined after 4.5 hr peptide stimulation.

(F) Phenotypic and functional analyses of D35 $TCR_{SV40\text{-}I}$ after PD1 and PD-L1 blockade in vivo. Top: Experimental scheme. Bottom: Expression levels of TBET, Ki67, PD1, TIM3, GZMB, and IFN-γ and TNF-α production (after 4.5 hr peptide stimulation). Each symbol represents an individual mouse. Data show mean ± SEM (p values are shown; ns, not statistically significant) using unpaired, two-tailed Student's t test (for analysis between isotype and treatment group).

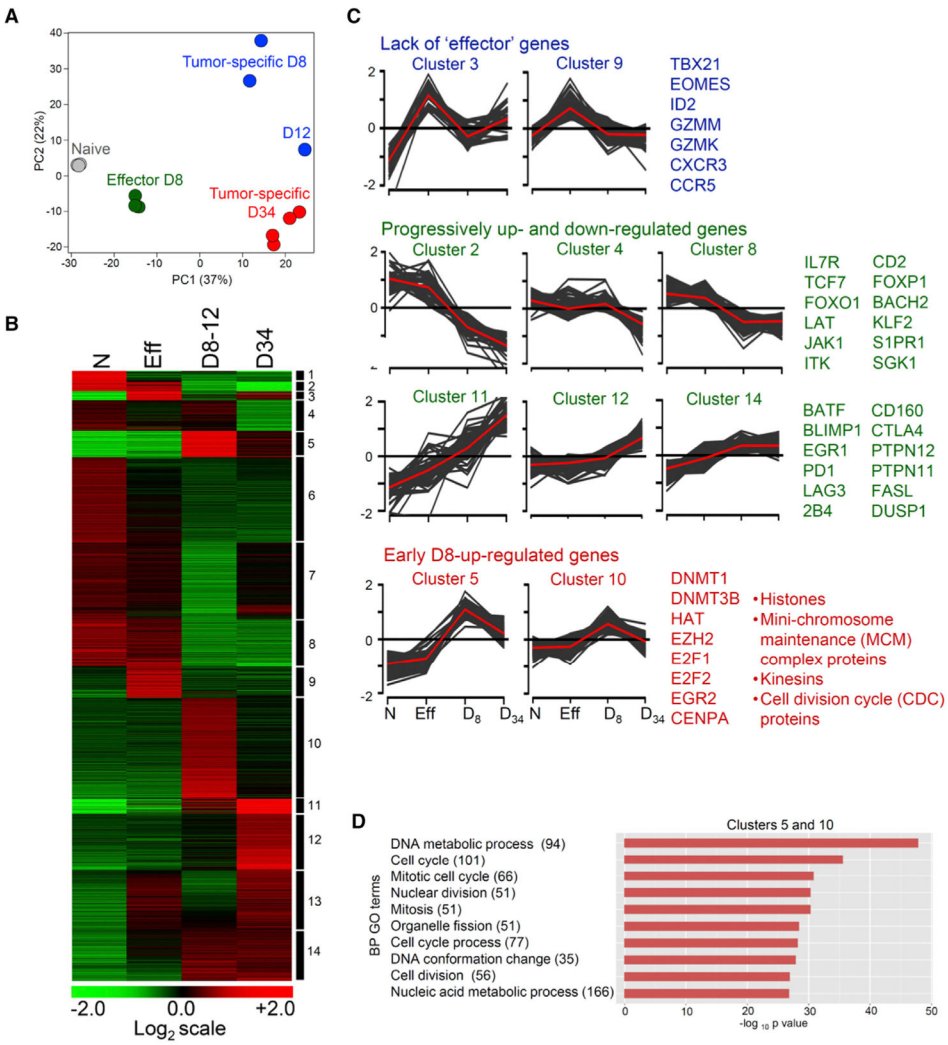

Figure 3. Genome-wide Transcriptome Analysis of Tumor-Specific $TCR_{SV40\text{-}I}$ $CD8^+$ T Cells in Pre-malignant Lesions

(A) Principal component analysis of D8–12 $TCR_{SV40\text{-}I}$ (n = 3) and D34 $TCR_{SV40\text{-}I}$ (n = 4) isolated from pre-malignant liver lesions, with naive (N; n = 3) and effector (Eff; n = 3) $TCR_{SV40\text{-}I}$ as controls.

(B) K-means clustering; heatmap of transcript levels for all 14 clusters show log_2-tranformed expression intensities that were mean-centered at the probe level.

(C) Selected K-means clusters. Lack of effector genes (blue, top); progressively up- or downregulated genes (green, middle); early, D8-upregulated genes (red, bottom).

(D) Top 10 biological processes (BP) (Gene Ontology [GO] terms) enriched in clusters 5 and 10. Numbers in parentheses indicate the numbers of genes within each GO term.

See also Figure S3 and Table S1; for (A) and (C), FDR *q* value ≤ 0.05.

A

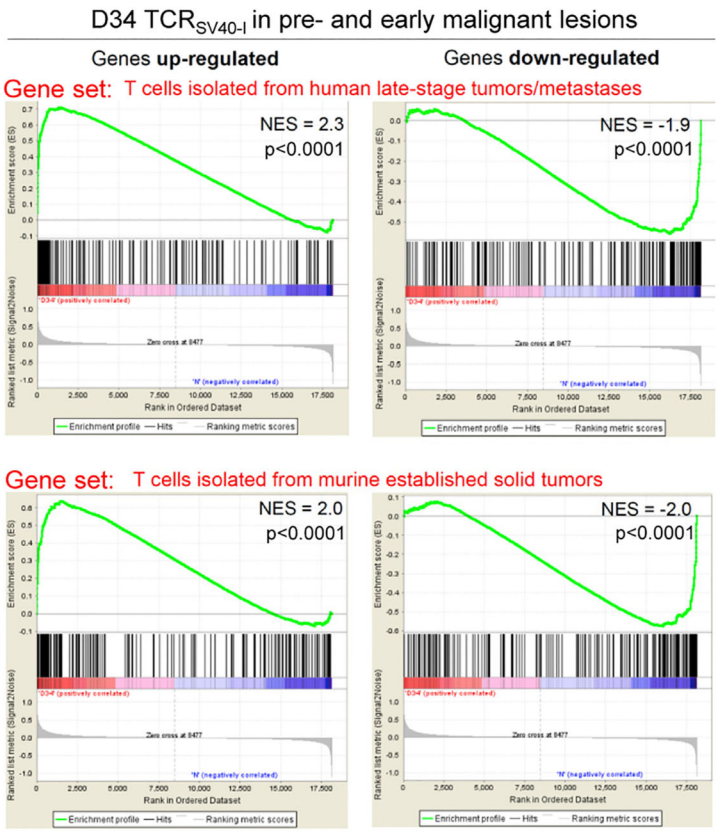

B

	Gene Names
Genes up	*Blimp1, Batf, Dusp1, Pd1, Tim3, Ptpn22, Ptprj, Id2, Ctla4, Lag3, Cd137, Fasl, Gapdh, Fyn, Rgs1, Rgs16, Nfat5, Nrp1, Klrd1, Kif11, Cd200*
Genes down	*Tcf7, Foxo1, Foxp1, Tcf12, Il7r, Lef1, Bach2, Itk, Ikzf1, Klf2, Klf7, Notch2, Mapk8, Sell, Jmjd1a, Satb1*

Figure 4. T Cells Isolated from Pre- and Early Malignant Lesions Exhibit the Molecular Hallmarks of T Cells from Late-Stage Human and Mouse Tumors

(A) Enrichment of genes sets in D34 TCR$_{SV40-I}$ from pre-malignant lesions described for T cells from late-stage and metastatic human tumors (GEO: GSE24536) (top) and mouse tumors (GEO: GSE42824) (lower). 200 most differentially expressed genes in T cells from human or mouse late-stage tumors (compared to naive T cells) were used for GSEA analyses of D34 TCR$_{SV40-I}$. NES, normalized enrichment score.

(B) Examples of genes enriched in D34 TCR$_{SV40-I}$.

See also Figure S4.

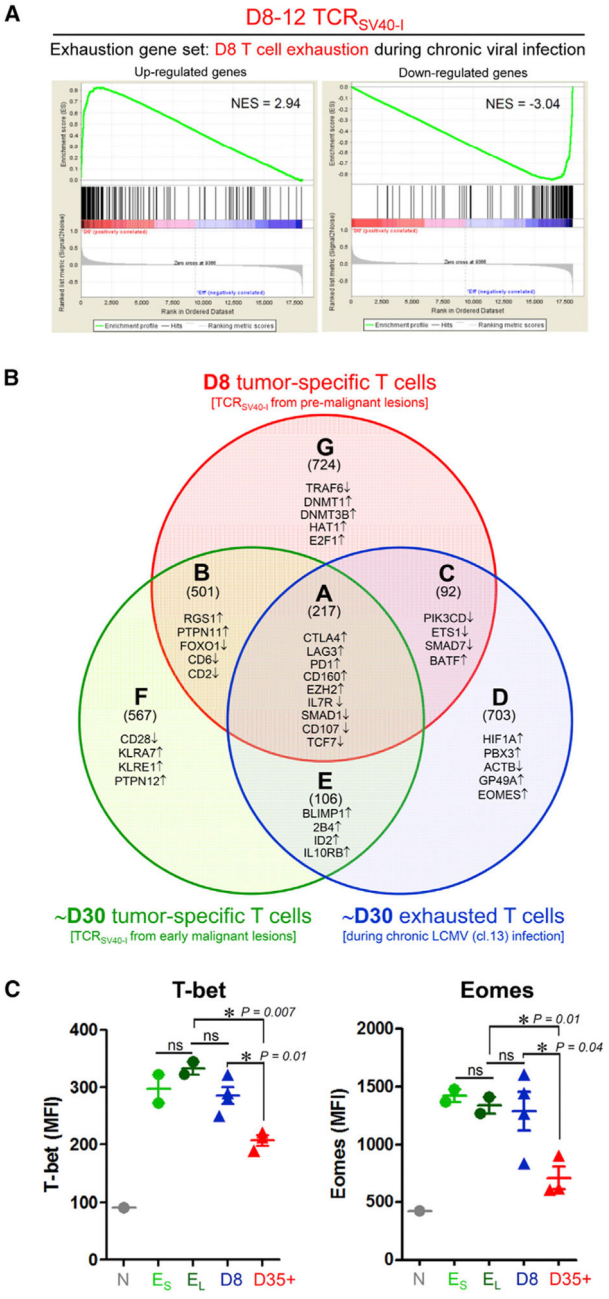

Figure 5. Tumor-Specific TCR_{SV40-I} T Cells and Exhausted Virus-Specific T Cells Share a Conserved Core Program of Dysfunction

(A) Gene set enrichment analysis (GSEA) in D8 TCR_{SV40-I} of "D8 exhaustion in chronic viral infection" genes (GEO: GSE30962). GSEA plot of D8 TCR_{SV40-I} (versus D8 Effectors) of genes previously identified to be upregulated (left) or downregulated (right) in exhausted, virus-specific T cells 8 days after chronic viral infection (compared to Effectors, 8 days after acute infection). NES, normalized enrichment score. See also Figure S5. FDR q value ≤ 0.001.

(B) Venn diagram of D8 $TCR_{SV40\text{-}I}$ (red) and ~D30 $TCR_{SV40\text{-}I}$ (green) from pre- and early malignant lesions and of ~D30 exhausted T cells during chronic viral LCMV infection (clone 13) (GEO: GSE9650). See Table S2 for full gene list.
(C) TBET and EOMES expression in naive (N), effectors from spleens and livers 8 days after *Listeria* immunization (E_S and E_L), and $TCR_{SV40\text{-}I}$ isolated from pre- and early malignant lesions at D8 and D35 after tumor initiation (D8, D35+). Each symbol represents an individual mouse; data show mean ± SEM. p values are shown.
See also Figure S5C.

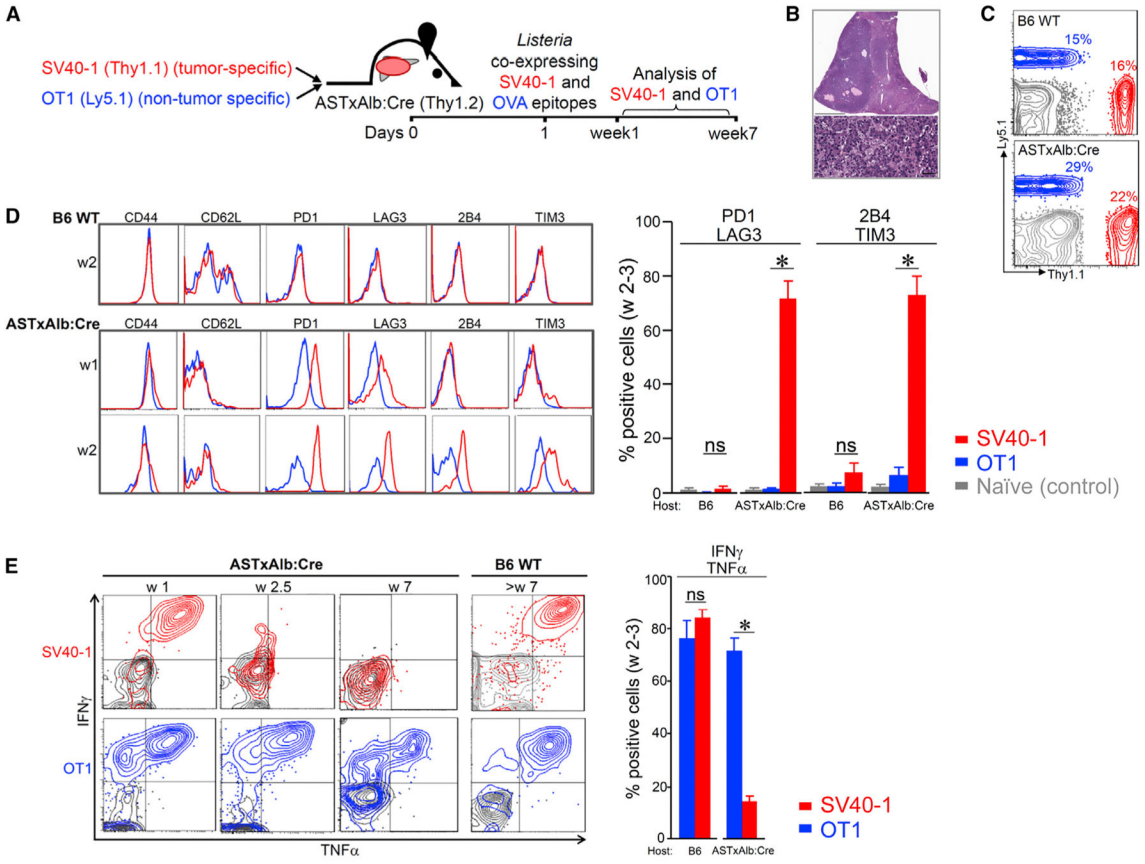

Figure 6. Persistent Antigen, Not the Microenvironment, Drives T Cell Dysfunction in Established, Solid Tumors

(A) Experimental scheme of co-transfer experiment.

(B) H&E staining of liver sections from ASTxAlb:Cre mice, showing hepatocellular carcinoma. Scale bar (top) represents 2 mm; scale bar (bottom) represents 50 μm.

(C) 1 week after infection with 5×10^6 cfu of LM-Tag-I-OVA, livers from ASTxAlb:Cre and spleens from B6 mice were analyzed for expansion of donor $TCR_{SV40\text{-}I}$ ($Thy1.1^+$) and $TCR_{OT\text{-}I}$ ($Ly5.1^+$) by FACS.

(D) Flow cytometric analysis of $TCR_{SV40\text{-}I}$ and $TCR_{OT\text{-}I}$ from livers (ASTxAlb:Cre) or spleens (B6) 1 week (w1) and 2 weeks (w2) after transfer and immunization. Histograms are gated on $CD8^+$ $Thy1.1^+$ and Ly5.1+ cells, respectively. Right: $TCR_{SV40\text{-}I}$ (red) and $TCR_{OT\text{-}I}$ (blue) isolated from B6 or ASTxAlb:Cre host mice 2–3 weeks after transfer; naive $TCR_{SV40\text{-}I}$ are shown as control (gray); *$p < 0.0001$ using unpaired, two-tailed Student's t test (for analysis between $TCR_{SV40\text{-}I}$ and$TCR_{OT\text{-}I}$, from 3–4 independent experiments, with n = 5–8).

(E) Intracellular IFN-γ and TNF-α production by $TCR_{SV40\text{-}I}$ and $TCR_{OT\text{-}I}$ isolated from livers (ASTxAlb:Cre) or spleens (B6) 1 (w1), 2.5 (w2.5), or 7 (w7) weeks after transfer. Results are representative of four independent experiments. Right: IFN-γ^+ and IFN-γ^+/TNF-α^+ $TCR_{SV40\text{-}I}$ (red) and $TCR_{OT\text{-}I}$ (blue) 2–3 weeks after transfer; *$p < 0.0001$ using

unpaired, two-tailed Student's t test (for analysis between SV40-1 and $TCR_{OT\text{-}I}$, from 2 independent experiments, with n = 2–4).